Available online at www.sciencedirect.com
ScienceDirect
Journal of Power Sources 160 (2006) 44–49
JOURNAL OF POWER SOURCES
www.elsevier.com/locate/jpowsour

Electrocatalytic oxidation of methanol on Pt modified single-walled carbon nanotubes

Dao-Jun Guo [a,b], Hu-Lin Li [a,*]

[a] College of Materials Science and Technology, Nanjing University of Aeronautics and Astronautics, Nanjing 210016, PR China
[b] College of Chemistry and Chemical Engineering, Lanzhou University, Lanzhou 730000, PR China

Received 30 November 2005; received in revised form 26 December 2005; accepted 6 January 2006
Available online 30 June 2006

Abstract

Platinum nanoparticles on modified single-walled carbon nanotubes (SWNT) were investigated by a completely new electrochemical method. A Pt(IV) complex was formed on the SWNT surface through coordination to the oxygen atom of an oxide functional group on the SWNT surface and then converted to platinum nanoparticles by a potential pulse method. The structure and chemical nature of Pt nanoparticles on SWNTs have been investigated by transmission electron microscopy and X-ray diffraction, the mean diameter of Pt nanoparticles was 5–8 nm. The electrocatalytic properties of the Pt/SWNT electrode for methanol oxidation and its kinetic characterization were investigated by cyclic voltammetry (CV) and excellent electrocatalytic activity was observed.

Keywords: Carbon nanotubes; Catalyst support; Electrochemical properties

1. Introduction

Methanol oxidation at platinum based electrodes has been extensively studied in the fuel cell context and is still a subject of interest [1–6], in spite of the intense research efforts in the last decade, the lack of efficient and inexpensive electrocatalysts remains one of the challenges to the implementation of low temperature fuel cells [7,8]. The major problems, which decrease the efficiency of conversion of the chemical energy of the methanol fuel to electrical energy in a DMFC, are the slow methanol electro-oxidation reaction kinetics at conventional Pt anode electrocatalysts. The poor kinetics of methanol oxidation at the anode is mostly due to self-poisoning of the surface by reaction intermediates such as CO, which are formed during dehydrogenation of the methanol [9]. Therefore, in order to improve the efficiency of the DMFC, anode electrocatalysts are required which combine a high activity for methanol dehydrogenation and an improved tolerance towards CO poisoning [7,10–12].

The tubular structure of carbon nanotubes makes them unique among different forms of carbon, and they can thus be exploited as an alternative material for catalyst support in heterogeneous catalysis [13] and in fuel cells [14–23]. But the inert, pristine surface of SWNTs makes a difficult substrate on which to attach metal, so oxidation is often attempted. Functionalization of carbon nanotubes by chemical oxidation using H_2SO_4/HNO_3, H_2SO_4/H_2O_2, HNO_3, O_3, $KMnO_4$, OsO_4 and RuO_4 has opened up new opportunities for carbon nanotube chemistry [24–30] and has the added advantage of being able to both modify and study nanotube properties in solution. Chemical oxidation generally results in the production of carboxylic groups at the defect sites located at the end and/or the sidewalls of nanotubes because of the different chemical reactivity between perfect structure and defects. But vigorous oxidation processes will often lead to damage of the tubes [31–34]. To avoid the harsh conditions of oxidative treatment, it is therefore important to develop good techniques to improve adhesion through surface modification of carbon nanotubes before metal nanoparticles deposition.

In the present study, we have developed a new method for the production of carboxylic groups at the defect sites located at the ends and/or the sidewalls of the nanotubes without the further damage of SWNTs via electrochemical process. And then the Pt nanoparticles were chose to deposit on the surface

* Corresponding author. Tel.: +86 931 8912517; fax: +86 931 8912582.
E-mail addresses: guodaojun03@163.com (D.-J. Guo), LHL_MSC@nuaa.edu.cn (H.-L. Li).

0378-7753/$ – see front matter © 2006 Elsevier B.V. All rights reserved.
doi:10.1016/j.jpowsour.2006.01.026

of SWNTs based upon the reported electrochemical deposition on the surface of other carbon substrate via formation of salt-like linkages with the carboxylic acid groups [35,36] by control the potential range. The electrocatalytic activity of a Pt/SWNT electrode for methanol oxidation was investigated in detail.

2. Experimental

2.1. Preparation of carbon nanotube paste (CNTP) electrode

SWNTs were produced via the chemical vapor deposition method [37]. The as-produced SWNTs were demineralized by magnetically stirring in a suitable amount of 12 M HCl for 24 h. This suspension was allowed to settle, the acid was decanted, and fresh acid solution was added. This procedure was repeated a minimum of three times for each SWNT sample. After the final acid treatment, the SWNTs were filtered and washed with distilled water until the filtrate was neutral. The SWNTs were dried at 80 °C in vacuum oven. This demineralization procedure removes the metallic (or bimetallic) catalyst that was used to prepare the SWNTs. In this way, only the subsequently added platinum metal can catalyze the methanol oxidation reaction.

Carbon nanotube paste electrode was prepared by mixing single-walled carbon nanotubes and mineral oil in a ratio 60.0% (w/w) carbon nanotubes and 40.0% (w/w) mineral oil. The paste was carefully hand-mixed in a mortar and then packed into a cavity (3-mm diameter, 2-mm depth) at the end of a Teflon tube. The electrode was provided by a copper wire connected to the paste in the inner hole of the tube. The paste was kept at room temperature in a desiccator until used.

2.2. Dispersion of Pt nanoparticles on SWNTs

The electrochemical synthesis of Pt nanoparticles on the SWNT surface, is a three-step processes: (1) potential cycling (500 mV s^{-1}) from +0.6 to +3.0 V was performed in 4.9 M H_3PO_4 solutions for 10 min in order to produce oxide functional groups (quinoid, carbonyl and carboxylate) at the defect sites located at the ends and/or the sidewalls of the carbon nanotubes; (2) octahedral complexes of Pt(IV) were formed on the SWNT surface from 2.5 mM K_2PtCl_4 + 0.1 M K_2SO_4 aqueous solutions by cyclic voltammetry (CV) under the condition of the potential range from 0.3 to 1.3 V at a sweep rate of 100 mV s^{-1}; (3) the surface complexes on the SWNTs can be converted to platinum nanoparticles by potential pulse method. The potential was stepped from +1.5 to −0.20 V in 0.1 M H_2SO_4 solutions for 100 ms.

2.3. Measurements

A conventional cell with three-electrode configuration was used throughout this work. A CNTP electrode was employed as working electrode. A platinum foil served as the counter electrode and a saturated calomel electrode (SCE) was used as the reference electrode. Electrochemical measurements were performed with BAS100B electrochemical analyzer, and

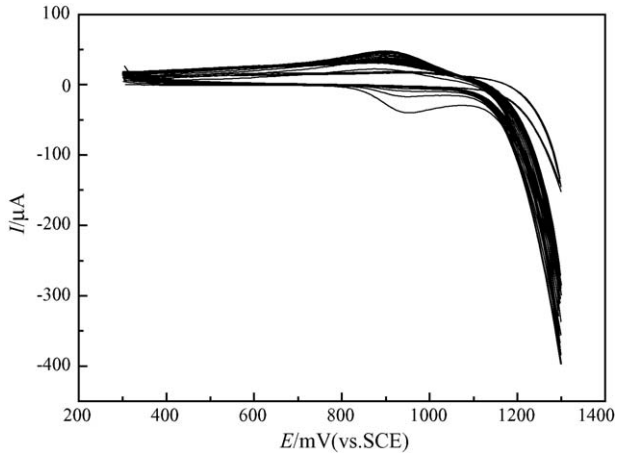

Fig. 1. Cyclic voltammograms of 2.5 mM K_2PtCl_4 in 0.1 M K_2SO_4 solution at a SWNT electrode; scan rate, 100 mV s^{-1}.

the potentials were measured and reported with respect to the SCE.

The morphology of synthesized nanoparticles was observed on a Hitachi600 transmission electron microscopy (TEM). The samples were prepared by dropping the Pt/SWNT composite ethanol solution on the carbon-coated Cu grids and observed at 100 kV.

X-ray diffraction (XRD) data of the samples were collected using a Rigaku D/MAX 24000 diffractometer with Cu Kα radiation.

3. Results and discussion

3.1. Preparation of Pt nanoparticles on SWNTs

Fig. 1 shows the typical cyclic voltammograms of a CNTP electrode in 2.5 mM K_2PtCl_4 + 0.1 M K_2SO_4 aqueous solutions. An irreversible anodic peak was observed around +1.0 V, corresponding to the oxidation of $PtCl_4^{2-}$, while the cathodic peak was sparingly evident. It is reasonable to suggest that oxygen atom of the functional group such as carboxylate serves as one of the two axial ligands when the planar complex of Pt(II) is oxidized to form the octahedral complex of Pt(IV), which is illustrated as following.

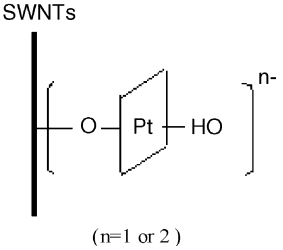

(n=1 or 2)

The complexes of Pt(IV) were precursors of Pt nanoparticles, which can be converted to platinum nanoparticles by potential pulse method. The potential was stepped from +1.5 to −0.20 V in 0.1 M H_2SO_4 solutions for 100 ms. A typical current–time transient seen for Pt(IV) modified SWNTs in 0.1 M H_2SO_4 solutions is shown in Fig. 2(curve A). Curve B represents the transient of

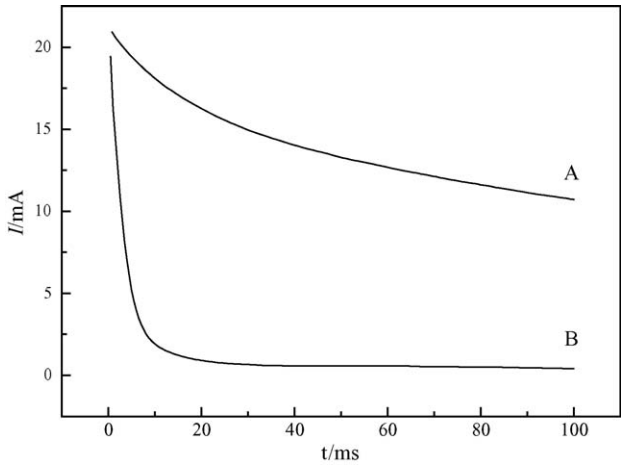

Fig. 2. Typical current–time transient of Pt(IV) grafted onto the SWNTs in 0.1 M H_2SO_4.

electrochemically pretreated SWNTs. Compared with the two curves, curve A exhibits a much larger current, which clearly shows that Pt(IV) has been coordinated and reduced on the SWNT surfaces.

3.2. Background cyclic voltammetry of Pt/SWNT composites

Background cyclic voltammograms for the Pt/SWNT composite electrode is presented in Fig. 3. The voltammograms were obtained in 1 M H_2SO_4 solution at a sweep rate of 50 mV s^{-1}. The voltammetric features of Pt/SWNT composites are characteristic of Pt metal, with Pt oxide formation in the +0.7 to +1.2 V region, the reduction of Pt oxide at ca. +0.5 V, and the adsorption and desorption of hydrogen between 0 and −0.18 V. This result suggests that the Pt particles are in good electronic contact with the SWNT surface.

The stability of the Pt deposits was investigated. Long-term potential cycling for the Pt/SWNT electrode between −0.2 and +1.0 V in 1 M H_2SO_4 was performed for 20 cycles. The maximum current density achieved at the upper and lower potential limit was ca. 1.63 mA. The voltammetric features were nearly identical before and after cycling, indicating the absence of any catalyst loss. The charge associated with desorption of hydrogen before cycling was 0.16 mC and after cycling actually increased to 0.25 mC. This increase indicates that the Pt deposits were not lost and the active catalyst area increased due to surface roughening during potential cycling.

The real surface area of platinum for the Pt/SWNT catalysts could be estimated from the integrated charge in the hydrogen absorption region of the cyclic voltammogram. The areas in m^2 were calculated from the following formula assuming a correspondence value of 0.21 mC (calculated from the surface density of 1.3×10^{15} atom per cm^2, a value generally admitted for polycrystalline Pt electrodes [38]) and the Pt loading S_{EL} (cm^2) = Q_H/0.21 mC. Q_H represents for charges exchanged during the electroadsorption of hydrogen on Pt; S_{EL} stands for real surface area obtained electrochemically.

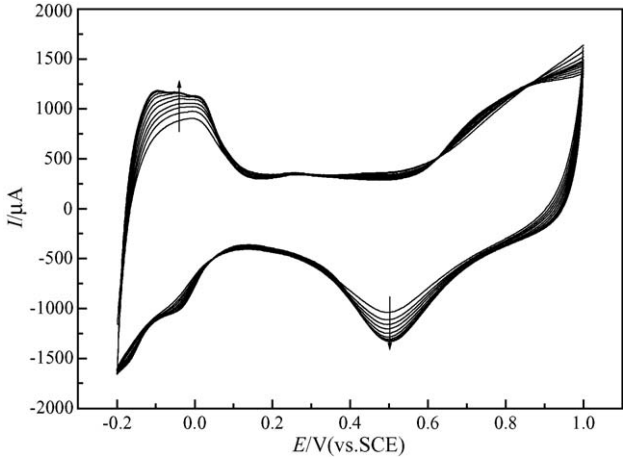

Fig. 3. Cyclic voltammograms of Pt/SWNT electrode. Electrolyte: 1 M H_2SO_4; sweep rate: 50 mV s^{-1}; geometric surface area: 0.09 cm^2.

3.3. TEM analysis and element composition of Pt/SWNT composites

The micrographs of Pt/SWNT composites have been investigated by TEM (Fig. 4). It can be seen that Pt nanoparticles were well dispersed in the Pt/SWNT composites with a diameter of 5–8 nm. These particles have attached selectively to SWNT surfaces respectively along the single bundles of CNTs. The large black blobs in the TEM image are the amorphous carbon produced in the process of preparing single-walled carbon nanotubes. In order to avoid the harsh conditions of oxidative treatment in the strong acid solution such as HNO_3, HNO_3/H_2SO_4 and so on, SWNTs were only demineralized in a suitable amount of 12 M HCl solution, the demineralization procedure only removes the metallic (or bimetallic) catalyst that was used to

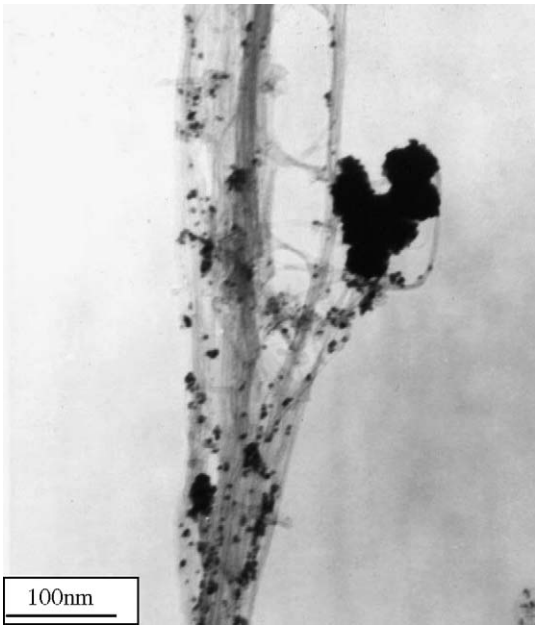

Fig. 4. Transmission electron micrograph (TEM) image of Pt/SWNT composites.

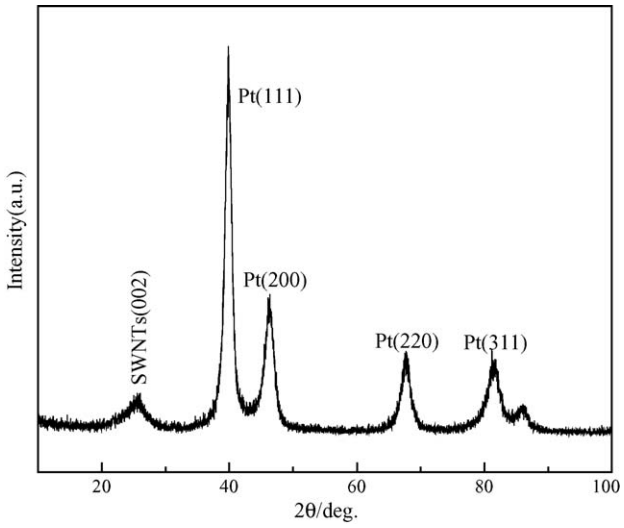

Fig. 5. Powder X-ray diffraction (XRD) pattern of Pt/SWNT composites.

produce the SWNTs. So there remains some amorphous carbon or carbon black in the sample.

3.4. XRD analysis of Pt/SWNT composites

The X-ray power diffraction (XRD) spectrum of Pt/SWNT composites is shown in Fig. 5. The SWNTs showed typical peak of (0 0 2) phase of SWNTs or graphite [39]. The peaks at 39.7°, 46.2°, 67.4° and 81.2° can be assigned to (1 1 1), (2 0 0), (2 2 0) and (3 1 1) crystalline plane diffraction peaks, respectively. The average size of the Pt particles is 5.7 nm calculated by the Scherrer formula, which is in good agreement with the results by the TEM image.

3.5. Electrochemical properties of Pt/SWNT composites

Fig. 6 shows the typical cyclic voltammograms of SWNT, Pt/SWNT paste electrodes in 2 M CH_3OH + 1 M H_2SO_4 aqueous solutions. For SWNT paste electrode, the background current (curve 1), which is the nature of the double layer capacitance, is much larger due to the high surface area of SWNT paste electrode. On the other hand, the oxidation and reduction peaks are observed obviously at 0.35 and 0.28 V (versus SCE), it may correlate with the redox behavior of the carboxylic acid groups [40], which implies that the surface of SWNTs has been activated by electrochemical treatment in 0.5 M H_3PO_4 solution mentioned above. But no current peaks of methanol oxidation are observed, which indicates that the SWNTs have no electrocatalytic activity for methanol oxidation. From curve 2 in Fig. 6, two peaks of methanol oxidation can be observed and the peak potentials (E_p) are 0.64 and 0.45 V, respectively. The potential of methanol oxidation are more negative than that of the other catalysts [41]. This may be attributed to the high dispersion of platinum catalysts and electrochemical treatment of SWNTs by which various oxide functional groups (e.g. quinoid, carbonyl and carboxylate) were produced on its surface. These surface groups may serve as "active oxygen" for the formation of CO_2. So the CO poisoned platinum can be regenerated via the reaction of surface CO with oxygen species on SWNTs to yield CO_2. Furthermore, the increased catalytic reactivity and lower self-poisoning ratios of the SWNT-supported platinum catalysts may be attributable to other various causes, including: (a) more efficient mechanisms for the removal of the adsorbed species; (b) increased electrical conductance of the SWNT when compared with the classical carbonaceous supports such as carbon black and so on; (c) decreased impurities in the carbon support; (d) the attainment of a preferred crystallographic orientation by the Pt particles as a result of the interaction with the SWNT substrate.

3.6. Kinetic characterization of methanol electro-oxidation on Pt/SWNT electrode

The cyclic voltammograms of 2 M CH_3OH in 0.5 M H_2SO_4 with different scan rates and different concentrations with the same scan rate at a Pt/SWNT electrode are presented in Figs. 7 and 8, respectively.

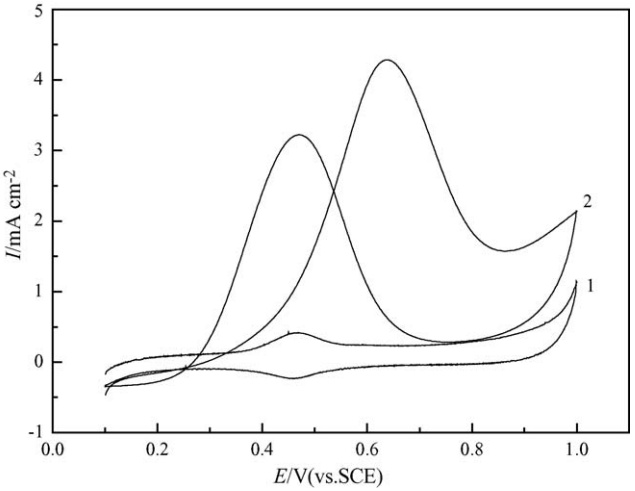

Fig. 6. Cyclic voltammograms of 2 M CH_3OH in 1 M H_2SO_4 at SWNT (1), Pt/SWNT (2) paste electrodes. Scan rate: 50 mV s^{-1}.

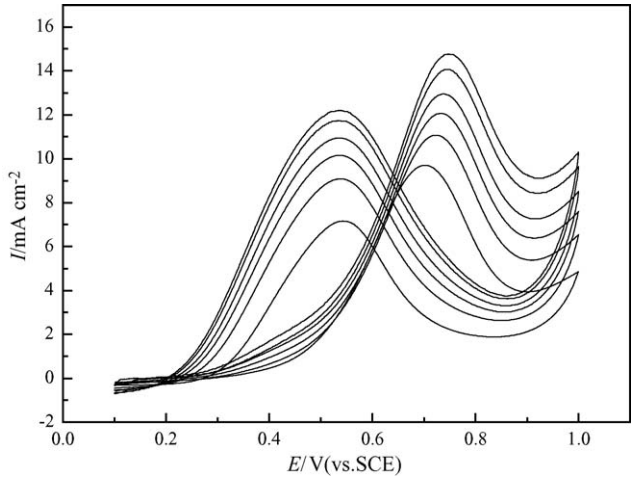

Fig. 7. Voltammograms of 2 mol L^{-1} CH_3OH in 0.5 mol L^{-1} H_2SO_4 solutions. Scan rate: 10, 30, 50, 70, 100,120 mV s^{-1} from inner to outer.

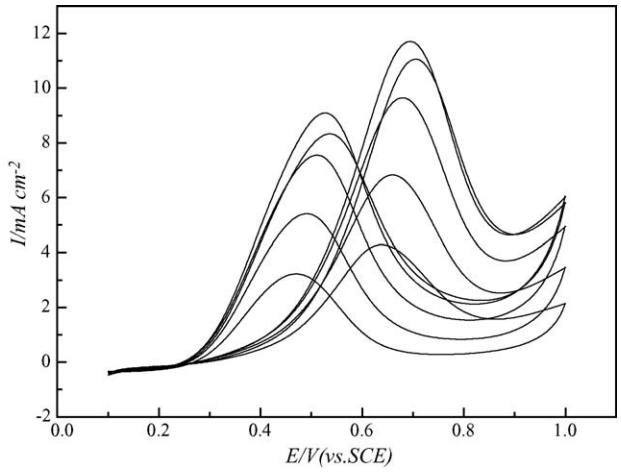

Fig. 8. The CV curves for methanol at a scan rate of 15 mV s^{-1} at various concentrations: 0.2, 0.5, 1.0, 1.5, 2.0 mol L^{-1} from inner to outer.

The relation between the peak current density obtained from forward CV scan and $\nu^{1/2}$ of CV is shown in Fig. 9, and a linear relationship is also observed. It can be obtained that the process of methanol oxidation may be controlled by diffusion of methanol [42]. Additionally, the peak potential (E_{pa}) (the forward a scan), increase with the increase of ν, and linear relationship can be obtained between E_p and $\log(\nu)$, as shown in Fig. 10. It indicates that the oxidation of methanol is an irreversible electrode process. For an irreversible charge transfer electrode process, the plot of E_p and $\ln(\nu)$ is a straight line with a slope $K = RT/2\alpha nF$ (where α stand for the electron transfer coefficient), from Fig. 10, we could obtain the slope of E_p versus $\log(\nu)$ is as following: $\partial E_p/\partial(\ln \nu) = 19.14$ mV, and we can calculated that $n\alpha = 0.66$. According to the relationship between peak current (i_p) and potential scan rate (ν), i.e., $i_p = 0.4958 \times 10^{-3} nF^{3/2}(RT)^{-1/2}(\alpha n)^{1/2} ACD^{1/2}\nu^{1/2}$ [43], (where i_p, A, D stand for peak current, electrode area and diffusion coefficient, respectively), the electron transfer numbers $n = 1.3$, according to the literature [44,45], hence $\alpha = 0.51$ can be obtained. The present results suggest that the chemisorbed poison are essentially linearly and bridge-bonded CO species when the value of $1 < n < 2$ according to Ref. [46]. When A, C (the concentration of substrate) are known, the diffusion coefficient $D = 7.45 \times 10^{-10}$ m^2/s at 293 K can be calculated from the plot of i_p versus $\nu^{1/2}$ for the oxidation peak shown in Fig. 9, which is accordance with Ref. [42].

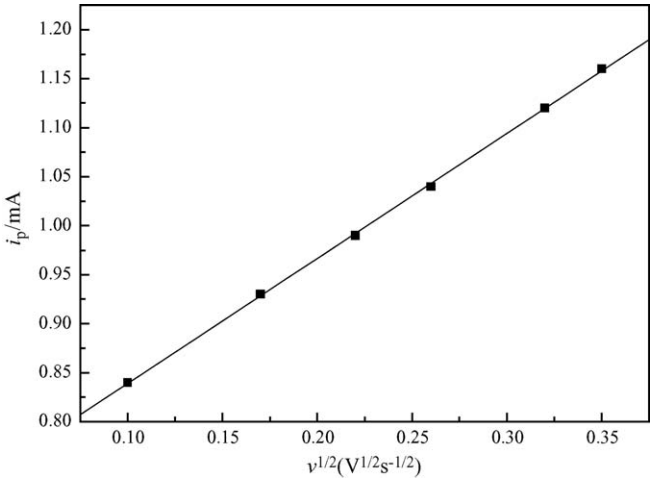

Fig. 9. The plot of peak current vs. square root of sweep rates. C_{CH_3OH} = 2 mol L^{-1}.

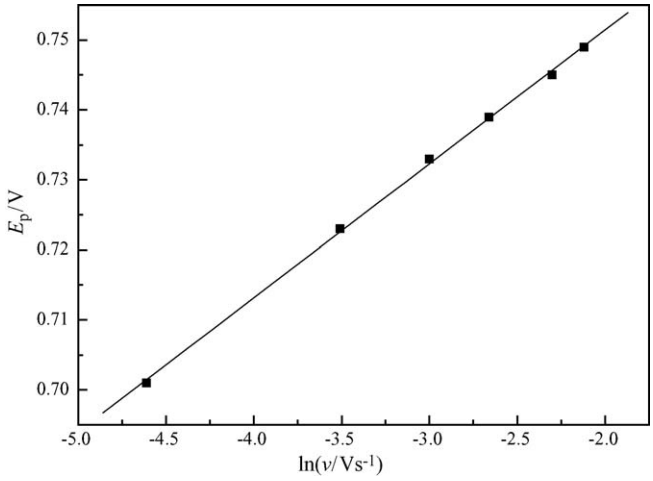

Fig. 10. The plot of E_{pa} vs. $\ln \nu$. $C_{CH_3OH} = 2$ mol L^{-1}.

4. Conclusions

The dispersion and electrocatalytic properties of platinum nanoparticles on SWNTs have been investigated. The Pt/SWNT composites show excellent electro-catalytic activity for methanol oxidation and have good stability. This may be attributed to the small particle size and chemical deposition of platinum on SWNTs. This also implies that SWNTs may be good candidates for catalyst supports because minimization of the precious metal catalyst (Pt) amounts in methanol oxidation is an important practical consideration in fuel cell technology.

References

[1] A. Kucernak, J.H. Jiang, Chem. Eng. J. 93 (2003) 81.
[2] M. Umeda, M. Kokubo, M. Mohamedi, I. Uchida, Electrochim. Acta 48 (2003) 1367.
[3] A.V. Tripkovic, K.D. Popovic, B.N. Grgur, B. Blinzanac, P.N. Ross, N.M. Markovic, Electrochim. Acta 47 (2002) 3707.
[4] J.B. Goodenough, A. Hamnett, B.J. Kennedy, R. Manoharan, S.A. Weeks, Electrochim. Acta 35 (1990) 199.
[5] A. Maruyama, I. Abe, Electrochim. Acta 48 (2003) 1443.
[6] M.S. Loffler, B. Gro, H. Natter, R. Hempelmann, Th. Krajewski, J. Divisek, Phys. Chem. Chem. Phys. 3 (2001) 333–336.
[7] S. Wasumus, A. Küver, J. Electroanal. Chem. 461 (1999) 14–31.
[8] G.J.K. Acres, J.C. Frost, G.A. Hards, R.J. Potter, T.R. Ralph, D. Thompsett, G.T. Burstein, G.J. Hutchings, Catal. Today 38 (1997) 393.
[9] J.-M. Leĭger, J. Appl. Electrochem. 31 (2001) 767.
[10] H.A. Gasteiger, N. Markovic, P.N. Ross, E.J. Cairns, J. Electrochem. Soc. 141 (1994) 1795.
[11] L. Dubau, C. Coutanceau, E. Garnier, J.-M. Leĭger, C. Lamy, J. Appl. Electrochem. 33 (2003) 419.
[12] R. Parsons, T. VanderNoot, J. Electroanal. Chem. 257 (1988) 9.
[13] N.M. Rodriguez, M.S. Kim, R.T.K. Baker, J. Phys. Chem. 98 (1994) 13108.
[14] G. Che, B.B. Lakshmi, E.R. Fisher, C.R. Martin, Nature 393 (1998) 346.
[15] G. Che, B.B. Lakshmi, C.R. Martin, E.R. Fisher, Langmuir 15 (1999) 750.

[16] B. Rajesh, V. Karthik, S. Karthikeyan, K.R. Thampi, J.M. Bonard, B. Viswanathan, Fuel 81 (2002) 2177.
[17] Z.L. Liu, X.H. Lin, J.Y. Lee, W.D. Zhang, M. Han, L.M. Gan, Langmuir 18 (2002) 4054.
[18] W.Z. Li, C.H. Liang, W.J. Zhou, J.S. Qiu, Z.H. Zhou, G.Q. Sun, J. Phys. Chem. B 107 (2003) 6292.
[19] T. Matsumoto, T. Komatsu, H. Nakano, K. Arai, Y. Nagashima, E. Yoo, T. Yamazaki, M. Kijima, H. Shimizu, Y. Takasawa, J. Nakamura, Catal. Today 90 (2004) 277.
[20] C. Kim, Y.J. Kim, Y.A. Kim, T. Yanagisawa, K.C. Park, M. Endo, M.S. Dresselhaus, J. Appl. Phys. 96 (2004) 5903.
[21] Yangchuan Xing, J. Phys. Chem. B 108 (50) (2004) 19255.
[22] C. Wang, M. Waje, X. Wang, J.M. Tang, C.R. Haddon, Y. Yan, Nano Lett. 4 (2) (2004) 345.
[23] M. Carmo, V.A. Paganin, J.M. Rosolen, E.R. Gonzalez, J. Power Sources 142 (2005) 169.
[24] D.B. Mawhinney, V. Naumenko, A. Kuznetsova, J.T. Yates Jr., J. Liu, R.E. Smalley, Chem. Phys. Lett. 324 (2000) 213.
[25] K.C. Hwang, J. Chem. Soc. Chem. Commun. 2 (1995) 173.
[26] J. Liu, A.G. Rinzler, H. Dai, J.H. Hafner, R.K. Bradley, P.J. Boul, A. Lu, T. Iverson, K. Shelimov, C.B. Huffman, F. Rodrigusz-Macias, Y.S. Shon, T.R. Lee, D.T. Colber, R.E. Smalley, Science 280 (1998) 1253.
[27] J. Chen, M.A. Hamon, H. Hu, Y. Chen, A.M. Rao, P.C. Eklund, R.C. Haddon, Science 282 (1998) 95.
[28] D.B. Mawhinney, V. Naumenko, A. Kuznetsova, J.T. Yates Jr., J. Liu, R.E. Smalley, J. Am. Chem. Soc. 122 (2000) 2383.
[29] K. Hernadi, A. Siska, L. Thien-Nga, Solid State Ionics 141 (2001) 203.
[30] T. Kyotani, S. Nakazaki, W.H. Xu, A. Tomita, Carbon 39 (2001) 782.
[31] E. Fitzer, R. Weiss, Carbon 25 (1987) 455.
[32] R.B. Mathur, J. Mittal, O.P. Bahl, N.K. Sandle, Carbon 32 (1994) 71.
[33] W.P. Hoffman, W.C. Hurley, T.W. Owens, H.T. Phan, J. Mater. Sci. 26 (1991) 4545.
[34] J.L. Kepley, A.J. Bard, Anal. Chem. 60 (1988) 1459.
[35] L. Xu, F.L. Li, S.J. Dong, J. Electroanal. Chem. 383 (1995) 133.
[36] F.L. Li, B.L. Zhang, S.J. Dong, E.K. Wang, Electrochim. Acta. 42 (1997) 2563.
[37] Q.W. Li, H. Yan, Y. Cheng, J. Zhang, Z.F. Liu, J. Mater. Chem. 12 (2002) 1179.
[38] T.R. Ralph, G.A. Hards, J.E. Keating, S.A. Campbell, D.P. Wilkinson, M. Davis, J. St-pierre, M.C. Johnson, J. Electrochem. Soc. 144 (1997) 3845.
[39] M. Terrones, W.K. Hsu, A. Schilder, H. Terrones, N. Grobert, J.P. Hare, Appl. Phys. A 66 (1998) 307.
[40] H.X. Luo, Z.J. Shi, N.Q. Li, Z.N. Gu, Q.K. Zhuang, Anal. Chem. 73 (2001) 915.
[41] K. Yahikozawa, Y. Fujii, Y. Mitlsuda, K. Nishimura, Y. Takasu, Electrochim. Acta 36 (1991) 973.
[42] K. Honda, M. Yoshimura, T.N. Rao, D.A. Tryk, A. Fujishima, J. Electroanal. Chem. 514 (2001) 35.
[43] A.J. Bard, L.R. Faulker (Eds.), Electrochemical Methods, 195, Chemical Industry Press, Beijing, 1984, p. 258.
[44] G.-Q. Lu, W. Chrzanowski, A. Wieckowski, J. Phys. Chem. B 104 (2000) 5566.
[45] T.D. Jarvi, S. Sriramulu, E.M. Stuve, J. Phys. Chem. B 101 (1997) 3649.
[46] J. Clavilier, S.G. Sun, J. Electroanal. Chem. 199 (1986) 187.